Multifractality in Rotational Percolation Models

Santanu Sinha and S. B. Santra

Department of Physics, Indian Institute of Technology

Guwahati, Guwahati-781039, Assam, India.

(Dated: July 15, 2008)

Abstract

In rotationally constrained percolation models, a site of a percolation cluster could be occupied more than once from different directions due to the nature of the rotational constraint. A state variable s_i is assigned to each lattice site whose value corresponds to the number times it has been visited during the growth of a cluster. It is proposed here that the percolation transition and the multifractal aspects of infinite percolation clusters under rotational constraint can be studied defining suitable measures in terms of the state variable s_i. This method does not require to introduce any external agency like an electric current or a random walker in order to explore multifractality as in the case of ordinary percolation. The state variable representation also describes the universality class of the percolation models appropriately.

I. INTRODUCTION

Multifractals appear in a wide range of situations like energy dissipation in turbulent flows[1], electronic eigenstates at metal insulator transition[2], diffusion in porous structures[3], diffusion limited aggregation[4], fluctuations in finance[5], dynamics of human heartbeat[6] and many others. The multifractal properties associated with the infinite percolation clusters at the percolation threshold p_c is considered in this paper. In ordinary percolation (OP)[7], a cluster is generated by occupying a lattice site randomly with a probability p or remains empty with a probability $(1-p)$. Each site of a percolation cluster then has two states, occupied or empty. The average q moments of the cluster size distribution of percolation clusters are linearly dependent on the moment q and described by a single fractal dimension d_f[8]. In order to study the multifractal aspects of percolation clusters, usually, a current distribution[9, 10] or a random walker[11] is introduced. However, in the presence of rotational constraint on the percolation model, an occupied site has always a direction associated with it and a site can be re-occupied from different directions. A site can be occupied at most z times from z different directions on a given lattice with coordination number z. There are two such well studied rotational percolation models exists, spiral percolation SP[12] and directed spiral percolation[13]. In these models, a state variable s_i then can be assigned to each lattice site and whose value will correspond to the number of times a site is visited during the growth of the cluster. The value of s_i then can change from 0 to 4 on a square lattice and 0 to 6 on a triangular lattice for SP and DSP models whereas it has only two states 1 and 0 in case of OP. In this paper, a new methodology is proposed to study the percolation transition in terms of the state variable s_i. Studying the physical properties associated with the state variable s_i, the percolation transition is possible to establish at the same percolation threshold p_c defined geometrically. The spanning clusters at $p = p_c$ are fractal. Distribution of s_i on the fractal substrate is very similar to mass distribution on a geometrical support usually taken for multifractal study[14]. In order to explore the multifractal aspects of the spanning percolation clusters in these rotationally constrained percolation models at $p = p_c$, it is now possible to define a suitable multifractal measure in terms of s_i. In this way, one does not need to introduce any other external agency like electric current or random walker in the model as it is usually done in the case of OP clusters. The variable s_i is inbuilt in the rotational models and represents an inherent

property of SP and DSP. It is found that the exponents associated with the q moments of the measure defined in terms of s_i are not limited by any linear dependence on the moment q for the rotational percolation models. It then indicates that the measure has multifractal character.

Below, description of the rotational percolation models will be given and the multifractal aspects of the spanning clusters will be investigated.

II. ROTATIONAL PERCOLATION MODELS

There are two well studied rotationally constrained percolation models, spiral percolation (SP)[12] and directed spiral percolation (DSP)[13]. In these models, clusters are grown following single cluster growth Monte Carlo (MC) algorithms. In these algorithms, the central site of the lattice is occupied with unit probability. The nearest neighbors of the central site is occupied with equal probability p in the first time step. As soon as a site is occupied, the direction from which it was occupied is assigned to it. Lists of eligible sites for occupation in the next MC time steps are identified and they are occupied with probability p. In these algorithms, an occupied site can be reoccupied from a different direction but it is forbidden for occupation from the same direction. Once a site is rejected for occupation it is forbidden for occupation throughout the simulation from any possible direction. Each MC time step can be considered as parallel update of nearest neighbours of already occupied sites. The growth of a cluster stops if there is no eligible site available for occupation. Identification of eligible sites for occupation in a MC step for SP and DSP are given below.

In SP, only a rotational field B is applied perpendicular to the plane (xy) of the lattice and directed along the negative z-axis (of a right handed coordinate system). As an effect of the B field, empty sites in the forward direction and in the clockwisely rotational direction are eligible for occupation. The forward direction is the direction from which the present site is occupied and the sense of rotational direction is defined with respect to the forward direction. The selection of eligible sites for occupation in SP model is demonstrated in Fig.1(a) for both the square and triangular lattices. There are two eligible sites on the square lattice and three eligible sites on the triangular lattice due to higher coordination number. The eligible sites are then occupied with probability p and the clusters grow isotropically on the lattice[12].

3

In case of DSP, a crossed directional field E is also applied in addition to the rotational field B. The E field is applied from left to right in the plane of the lattice and B is, as usual, directed along the negative z axis. Due to E field, empty site on the right of an occupied site is eligible for occupation along with the eligible sites for occupation due to B field. The selection of eligible sites for occupation in DSP model is demonstrated in Fig.1(b) for both the square and triangular lattices. The components of the directional constraint remain the same on both the lattices whereas there is an extra component of rotational constraint on the triangular lattice as in SP. The eligible sites are then occupied with probability p. Once a site is rejected for occupation it is forbidden for occupation throughout the simulation from any possible direction due to both E and B fields. Because of the simultaneous presence of both the E and B fields crossed to each other, a Hall field E_H appears in the system perpendicular to both E and B. As a result, an effective directional constraint E_{eff} acts on the system along the diagonal from left upper to right lower corner of the lattice. Here, the clusters grow anisotropically along the effective field E_{eff}[13].

The coordinate of an occupied site in a cluster is denoted by (x,y). Periodic boundary conditions are applied in both directions and the coordinates of the occupied sites are adjusted accordingly whenever the boundary is crossed. At each time step the span of the cluster in the x and y directions $L_x = x_{max} - x_{min}$ and $L_y = y_{max} - y_{min}$ are determined. If L_x or $L_y \geq L$, the system size, then the cluster is considered to be a spanning cluster.

Since an occupied site can be reoccupied from different directions due to the presence of rotational constraint in both the models, a site then can be occupied at most z times from z possible directions on a given lattice where z is the coordination number of the lattice. The value of z is 4 on the square lattice and it is 6 on the triangular lattice. This is unlike in the case of the ordinary percolation where a site is occupied only once. It is an essential and a special feature of SP and DSP models. It is thus possible to assign a state variable s_i to each site and the value of s_i will represent the number of times a site is occupied or visited. Initially the values of s_i are all set to zero. As soon as a site is occupied from any direction, the value of s_i is increased by 1. The values of the state variable is then given by $s_i = 0, \cdots, z$ on a given lattice. $s_i = 0$ corresponds to unoccupied site. The state variable s_i here is similar to the Ising spins with $(z + 1)$ states. In case of OP, s_i could have values only 0 and 1 corresponding to unoccupied and occupied sites.

Percolation clusters are generated here in the presence of rotational constraint on the

square and triangular lattices of size $L = 1024$ for both SP and DSP models. The percolation transition will be established first at the original p_c by calculating "spontaneous magnetization" in terms of s_i. The multifractal aspects of the measure distribution on the spanning clusters, defined in terms of s_i, are then investigated for both isotropic SP and anisotropic DSP clusters at $p = p_c$. The cluster properties are averaged over 5×10^4 spanning clusters.

III.   PERCOLATION THRESHOLD AND SPANNING CLUSTERS

Geometrically, the critical percolation probability p_c is the maximum probability below which no spanning cluster appears. At $p = p_c$, a spanning cluster appears for the first time in the system. In single cluster growth approach, the threshold p_c is generally identified by measuring the probability to have a spanning cluster (P_∞) as a function of p, the occupation probability. P_∞ goes to zero continuously as p tends to p_c from above. In the state variable formalism, the value of p_c can be identified in terms of "spontaneous magnetization" $M(p)$ defined in terms of the state variable s_i. $M(p)$ is defined as

$$M(p) = \frac{1}{N_{tot}} \sum_{j=1}^{N_{tot}} m_j(p), \qquad m_j(p) = \frac{1}{L^2} \sum_{i=1}^{L^2} s_i(p) \tag{1}$$

where L is the lattice size and N_{tot} is the total number of spanning clusters generated. $m_j(p)$ represents the magnetization per site for the jth spanning cluster generated using single cluster growth method. At $p = 1$, all the sites of an infinite cluster are expected to be occupied z times where z is the coordination number of the lattice and the size of the infinite cluster will be of the order of L^2, square of the system size. Thus, $M(1)$ is equal to z. As p tends to the percolation threshold p_c from above, $M(p)$ is expected to go to zero continuously from its maximum value z at $p = 1$ not only because the sites will be occupied less number of times but also the spanning cluster will disappear. $M(p)$ is measured on the square lattice ($z = 4$) for DSP model and it is plotted against p in Fig.2. It can be seen that it is going to zero at $p = p_c$ as expected and the value of p_c is the same as that determined by geometrical approach $p_c = 0.6550 \pm 0.0005$[13]. It is also expected that $M(p)$ becomes singular at $p = p_c$ with an exponent β as $M(p) \approx (p - p_c)^\beta$. In the inset of Fig.2, the power law has been verified and the exponent β is determined approximately as $\beta \approx 0.32$, close to the already obtained value (0.31 ± 0.01)[13]. The state variable formalism

of the rotationally constrained percolation models is then consistent with that of the usual geometrical approach. The value of p_c has also been recovered within error bar in the case of SP. Other critical properties of the models can also be identified in terms of the state variable s_i and a scaling theory is possible to develop.

Typical spanning clusters at $p = p_c$ generated on the square lattice of size $L = 2^6$ are shown in Fig.3(a) for SP and in Fig.3(b) for DSP. Different values of the state variable s_i is represented by different symbols as $s_i = 0$ (white space), $s_i = 1$ (filled circle), $s_i = 2$ (plus), $s_i = 3$ (filled triangle) and $s_i = 4$ (filled square). It can be seen that not only the state variables s_i are randomly distribution of over the spanning cluster but also the higher states form small islands allover the spanning cluster. This is similar to the situation of mass distribution on a geometrical support generally taken for multifractal study[14]. However, the state distribution over the spanning cluster is not a simple iterative process of mass distribution over a geometrical support. The spanning clusters consist of subsets of sites occupied once, twice upto a subset of sites occupied z times where z is the coordination number of the lattice considered. A particular subset may appear several times in a spanning cluster at different stages of growth of the cluster during a large number of MC steps. A multiplicative cascade of these subsets is then formed in a complicated manner during the growth of the cluster. The s_i distribution on the spanning cluster is then expected to have many folds. It is then interesting to investigate the moments of the s_i distribution over fractal objects, the spanning clusters here. It could also be noted that the SP cluster is compact and isotropic but the DSP cluster is highly rarefied and anisotropic. The elongation of the DSP cluster is along the effective field E_{eff} appeared in the system. However, the clusters are not merely DP clusters along E_{eff}. It has already been found that both SP and DSP belong to new universality classes than that of DP or OP[12, 13]. The fractal dimension d_f of the spanning clusters were found as $d_f \approx 1.733$[13] for DSP and ≈ 1.957[12] for SP. Geometrical properties of the percolation clusters are governed by this single exponent d_f. However, in the following it will be demonstrated that a measure defined in terms of the state variable s_i is not restricted by a single exponent rather needs a sequence of fractal dimensions to characterize the measure.

IV. MULIFRACTALITY

In order to study multifractality a suitable measure has to be defined. In general, a multifractal measure is related to the distribution of a physical quantity on a geometrical support [14]. The geometrical support here is the spanning percolation cluster at $p = p_c$ for the rotationally constrained percolation models. The distribution of the relative probability of a state over fractal substrates is a possible multifractal measure here. It is similar to the mass distribution on a geometrical support. The multifractal measure μ_i is then defined as

$$\mu_i = s_i / \sum_{i=1}^{L^2} s_i \qquad (2)$$

where s_i is the state variable associated with each lattice site. μ_i can be called as relative state variable. Note that the measure μ_i is normalized to unity when summed over the whole lattice. The maximum value of the measure is $\mu_{max} = z / \sum s_i$ and the minimum non-zero measure is $\mu_{min} = 1 / \sum s_i$ where z is the coordination number of the lattice. To obtain the multifractal nature of the distribution μ_i, it is necessary to study the scaling of the q-moments of the measure over different length scales on the geometrical support. If the measure μ_i is multifractal and the support is divided into n_ϵ boxes of size ϵ, then the weighted number of boxes $N(q,\epsilon)$ is given by

$$N(q, \epsilon) = \sum_{j=1}^{n_\epsilon} \mu_j^q \approx \epsilon^{-\tau(q)} \qquad (3)$$

where μ_j is the sum of the relative state variable in the jth box. Here $\tau(q)$ can be called as "state exponent". The weighted number of box $N(q, \epsilon)$ is determined as a function of the box size ϵ using box counting method for a given q. The boxes with at least one occupied site are only considered. The weighted number of boxes $N(q, \epsilon)$ are plotted against the box size ϵ for $q = -5$ to $q = +5$ for SP in Fig.4(a) and for DSP in Fig.4(b) generating spanning clusters on the square lattice of size $L = 1024$. It can be seen that the slopes of the plots change continuously for positive q up to $q = 0$. For $q < 0$, it seems that the usual box counting method adopted here is not working. The values of $N(q, \epsilon)$ remain unchanged over several box sizes ϵ starting from the smallest box size for a given q in both the models. It is expected that the plot should follow a straight line passing through the points at $\epsilon = 1$ and $\epsilon = 2^{10}$, the system size, in log-log scale since these two extreme points are not effected by the box size. It is shown by dashed lines for $q = -5$ in both the plots. It is observed that the value

7

of $N(q, \epsilon)$ jumps suddenly when the box size is reduced less than one quarter of the system size. This is due to the fact that at this box size there is at least one box appearing with a small measure and consequently the sum in Eq.3 diverges due to negative moment. The appearance of large box sizes with small measures is because of the fact that the spanning percolation clusters contain holes of all possible sizes. Difficulties in determining weighted number of boxes for $q < 0$ for the measure distribution on random structures are already reported in the literature[15]. The slopes of the plots in Fig.4 also remain almost unchanged with the moment q for $q < 0$. The weighted number of boxes has increased proportionally with higher negative moments. It has been verified that the estimation of $\tau(q)$ by fitting only through the smaller box sizes leads to a discontinuity in the plot of $\tau(q)$ versus q which is expected to be a smooth function of q. Discontinuity in the plot of $\tau(q)$ versus q was also observed in the cases of resistance fluctuations in randomly diluted networks [9] and in diffusion limited aggregation [16]. In these cases, there are breakdown of multifractal characters for negative moments due to exponential decay of the smallest measures.

Multifractal characteristics of the spanning clusters of rotationally constrained percolation models are then analyzed here taking large positive moments, changing q from 0 to 32. Analysis has been made on the square and triangular lattices of size $L = 1024$ for both SP and DSP models and the results are compared with that of the OP model. In Fig.5, $\tau(q)$ is plotted against q, (a) for SP model and $(b)$for DSP model. In both the plots the squares represent the square lattice data and the triangles represent the triangular lattice data. Circles represent the data obtained for OP model. It is found that $\tau(0)$ is $\approx d_f$, the fractal dimension of the corresponding spanning clusters and $\tau(1)$ is ≈ 0 here for all three models, OP, SP and DSP. $\tau(0)$ corresponds to the dimension of the support which are the spanning percolation clusters of different models considered here and $\tau(1)$ is zero because $\sum_i \mu_i = 1$. It is interesting to notice that the values of $\tau(q)$ for DSP and SP model depend on the moment q in a nonlinear way for positive moments. If the measure μ_i is characterized by a single fractal dimension d_f, the state exponent $\tau(q)$ should have a constant gap between two consecutive exponents[8] and consequently should have a linear dependence on q. In that case, a relationship between $\tau(q)$ and q in terms of d_f can be obtained as

$$\tau(q) = -(q - 1)d_f. \tag{4}$$

This relation is shown in Fig.5 by a solid line for OP taking $d_f = 91/48 \approx 1.896$. The

values of $\tau(q)$ obtained numerically for OP (circles) considering a two state model for which $s_i = 0$ and 1 are in good agreement with with Eq.4. There are few more things to notice. First, the state exponents of OP obey the constant gap equation given in Eq.4 as expected. The constant gap scaling was also observed for the mean number of distinct sites visited by a random walker on spanning percolation cluster by Murthy *et al*[17]. As a consequence, the measure distribution is mono-fractal. Second, the values of $\tau(q)$ for SP and DSP are deviated form straight line behaviour and have non-linear dependence on the moment q. Thus, each moment of the measure μ_i needs a new exponent to characterize in these models. Third, the functional dependence of $\tau(q)$ on q is found different for all three models. This is expected because the models, OP, SP and DSP, belong to different universality classes. Fourth, the $\tau(q)$ values on the square and triangular lattices are almost the same for the SP model whereas they are considerably different for the DSP model. This is also in agreement with the fact that the critical properties hold universality in the SP model whereas there is a breakdown of universality in DSP model between the square and triangular lattices in two dimensions[19]. Finally, the fact that a sequence of exponents is required to characterize the moments of the measure confirms the multifractal nature of μ_i distribution in SP and DSP models. It should be noted here that in SP and DSP the spanning clusters consist of four or six subsets depending on the number of nearest neighbours on a given lattice. The values of $\tau(q)$ then may be possible to obtain in terms of the fractal dimensions of the subsets consisting the spanning cluster coupled with a nonlinear dependence on q. However, it is difficult to determine the fractal dimensions of the individual subsets as they are generally small isolated islands in a spanning cluster as well as the nonlinear nature of $\tau(q)$.

The associated fractal dimensions $f(\alpha)$ with the measure and the corresponding Lipschitz-Hölder exponent α can be obtained through a Legendre transformation [18] of the sequence $\tau(q)$. The Legendre transformation is given below

$$\alpha(q) = -\frac{d\tau(q)}{dq}, \qquad f(\alpha) = q\alpha(q) + \tau(q). \tag{5}$$

The fractal dimensions $f(\alpha)$ are plotted against α in Fig.6. The values of $f(\alpha)$ obtained for SP clusters are shown in Fig.6 (a) and that of the DSP clusters are shown in Fig.6 (b). Since in the case of OP, the state exponent follows a constant gap equation (Eq.4) it is expected that $f(\alpha)$ versus α will be represented by a point $f(\alpha) = \alpha = d_f$. It is shown by an open circle in Fig.6. It has been verified measuring slopes at different regions of $\tau(q)$

9

versus q for OP that the slopes remain within the error bar of the point shown. In the cases of SP and DSP, spectra of $f(\alpha)$ against α are obtained because $\tau(q)$ has a non linear dependence on q. The symbols square and triangle correspond to the square lattice and the triangular lattice data respectively. There are few things to observe. First, $f_{max}(\alpha)$ corresponds to d_f of the respective models. Second, the $f(\alpha)$ curves are always $\leq d_f$ since the supports are spanning percolation clusters of fractal dimension d_f. Third, the spectrum of fractal dimensions $f(\alpha)$ for SP and DSP are found different. It means that not only the mass fractal dimension d_f is different but also the whole set fractal dimensions $f(\alpha)$s are different. It is expected because SP and DSP belong to different universality classes. Fourth, in case of SP, the spectrum of $f(\alpha)$ for the square lattice is identical with that of the triangular lattice for lower moments (starting from the same mass fractal dimension) and slightly different at large positive moments. In case of DSP, the spectra of $f(\alpha)$ on the two lattices are considerably different over the full range of positive moments considered here, starting from two different mass fractal dimensions. This again confirms the universality of critical exponents in SP and breakdown of universality of critical exponents in DSP between square and triangular lattices in two dimensions[19]. Fifth, the values of $f(\alpha_{min})$ for both SP and DSP clusters are not equal to zero. This means that in these cases, the rarest regions of measure μ_{max} distribution are still fractal in the limit $q \to \infty$. It is evident from the spanning clusters configurations given in Fig.3 that the μ_{max} distribution appears in small islands allover the spanning clusters and not as a point distribution. The fractal dimension of μ_{max} distribution of SP clusters is found little higher than that of DSP clusters. This is due to the presence of an extra directional constraint in the DSP model which takes the growth of the cluster away from a μ_{max} point whereas due to pure rotational constraint in the SP model the probability of growth around a μ_{max} point is little higher in comparison to DSP. It can also be noticed that, in case of DSP, the whole $f(\alpha)$ spectrum is shifted upward in order to match with the mass fractal dimension of the spanning DSP clusters on the triangular lattice. However this is not the case in SP model. Finally, the values of $f(\alpha)$ converges at a minimum of Lipschitz-Hölder exponent α_{min}. The Lipschitz-Hölder exponent $\alpha(\xi)$ is defined as $\mu_\xi = \delta^{\alpha(\xi)}$ where $\mu_\xi = \mu(\xi + \delta) - \mu(\xi)$ is the increment in the measure over a length ξ to $\xi + \delta$ [14]. The α_{min} value corresponds to the minimum of ξ, the length scale associated with μ_{max} clusters in this case. It could also be noticed that in both SP and DSP, the values of α_{min} on the triangular lattice is found little higher than that of the

square lattice. This is due to the fact that the number of μ_{max} points are generally higher on the triangular lattice than that on the square lattice.

V. CONCLUSION

Using the concept of state variable, the percolation transition in rotationally constrained models is established at the same percolation threshold p_c defined geometrically. A relative state variable is defined to study the multifractal aspects of the spanning clusters at $p = p_c$. It is found that the q-moments of the measure is characterized by a sequence of "state exponents" $\tau(q)$ for both SP and DSP. The existence of a sequence of state exponents confirms the multifractal character of the distribution of relative state variable on the infinite clusters of SP and DSP. The OP spanning clusters are not found multifractal in this measure. Taking Legendre transformation of $\tau(q)$, different spectra of associated fractal dimensions $f(\alpha)$ as a function of Lipschitz-Hölder exponents α are obtained. The universality of critical exponents in SP and breakdown of universality in DSP are also confirmed by the multifractal spectrum of fractal dimensions. The formalism of state variable is thus found suitable for studying percolation transition and multifractal aspects of certain percolation models.

[1] B. B. Mandelbrot in *Statistical Model of Turbulence* edited by M. Rosenblatt and C. Van Atta, Lecture notes in Physics, **12**, (Springer, New York, 1972).

[2] F. Milde, R. A. Römer, and M. Schreiber, Phys. Rev. B **55**, 9463 (1997); B. Huckestein and R. Klesse, Phil. Mag. B **77**, 1181 (1998); S. M. Nishigaki, Phys. Rev. E. **59**, 2853 (1999).

[3] S. B. Santra and B. Sapoval, Fractals **13**, 9 (2005).

[4] M. H. Jensen, A. Levermann, J. Mathiesen and I. Procaccia, Phys. Rev. E **65**, 046109 (2002).

[5] J. P. Bouchaud, M. Potters and M. Meyer, Eur. Phys. J. B **13**, 595 (2000); J-F Muzy, D. Sornette, J. Delour and A. Arneodo, Quantitative Finance **1**, 131 (2001).

[6] P. Ch. Ivanov, L. A. Nunes Amaral, A. L. Goldberger, S. Havlin, M. G. Rosenblum, Z. R. Struzik and H. E. Stanley, Nature **399**, 461 (1999); P. Ch. Ivanov, L. A. Nunes Amaral, A.

L. Goldberger, S. Havlin, M. G. Rosenblum, H. E. Stanley and Z. R. Struzik, Chaos **11**, 641 (2001).

[7] A. Bunde and S. Havlin, in *Fractals and Disordered Systems*, edited by A. Bunde and S. Havlin (Springer-Verlag, Berlin, 1991); K. Christensen and N. R. Moloney, *Complexity and Criticality*, (World Scientific, London, 2005).

[8] D. Stauffer and A. Aharony, *Introduction to Percolation Theory*, 2nd edition, (Taylor and Francis, London, 1994).

[9] R. Blumenfeld, Y. Meir, A. Aharony and A. B. Harris, Phys. Rev. B **35**, 3524 (1987).

[10] O. Stenull and H. K. Janssen, Europhys. Lett. **55**, 691 (2001).

[11] A. Bunde, S. Havlin and H. E. Roman, Phys. Rev. A **42**, 6274 (1990); E. Eisenberg, A. Bunde, S. Havlin and H. E. Roman, Phys. Rev. E **47**, 2333 (1993).

[12] P. Ray and I. Bose, J. Phys. A **21**, 555 (1988); S. B. Santra and I. Bose, J. Phys. A **24**, 2367 (1991).

[13] S. B. Santra, Eur. Phys. J. B **33**, 75 (2003), Int. J. Mod. Phys. B, **17** 5555 (2003).

[14] J. Feder, *Fractals*, (Plenum Press, New York and London 1998).

[15] A. block, W. von Bloh and H. J. Schellnhuber, Phys. Rev. A, **42**, 1869 (1990); P. Grassberger, Int. J. Mod. C **4**, 515 (1993); M. Yamaguti and C. P. C. Prado, Phy. Rev. E, **55**, 7726 (1997).

[16] J. Lee and H. E. Stanley, Phys. Rev. Lett. **61**, 2945 (1988); R. Blumenfeld and A. Aharony, Phys. Rev. Lett. **62**, 2977 (1989).

[17] K. P. N. Murthy, L. K. Gallos, P. Argyrakis and K. W. Kehr, Phys. Rev. E **54**, 6922 (1996).

[18] C. J. G. Evertsz and B. B. Mandelbrot, in the appendix of *Chaos and Fractals* by H. O. Peitgen, H. Jürgens and D. Saupe (Springer, New York, 1992).

[19] S. Sinha and S. B. Santra, Eur. Phys. J. B. **39**, 513 (2004); S. Sinha and S. B. Santra, Int. J. Mod. Phys. C **16**, 1251 (2005).
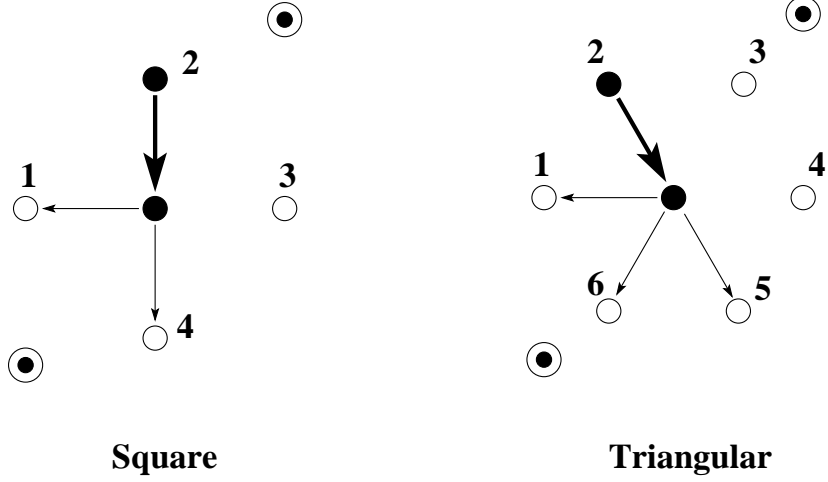
(a) SP model
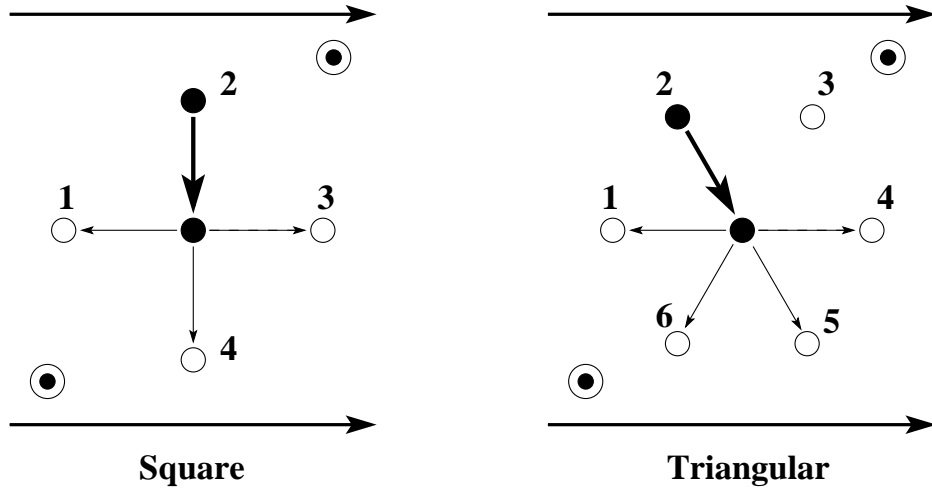
(b) DSP model

FIG. 1: Selection of empty nearest neighbours in a MC step in (a) SP model and (b) DSP model on the square and triangular lattices. Black circles are the occupied sites and the open circles are the empty sites. Thick long arrows from left to right represent directional constraint (E). The clockwise rotational constraint (B) is shown by encircled dots. The central site here is occupied from site 2 and shown by short thick arrows. The eligible sites for occupation due to E field are shown by dotted arrows and thin solid arrows indicate the same due to B field on both the lattices.
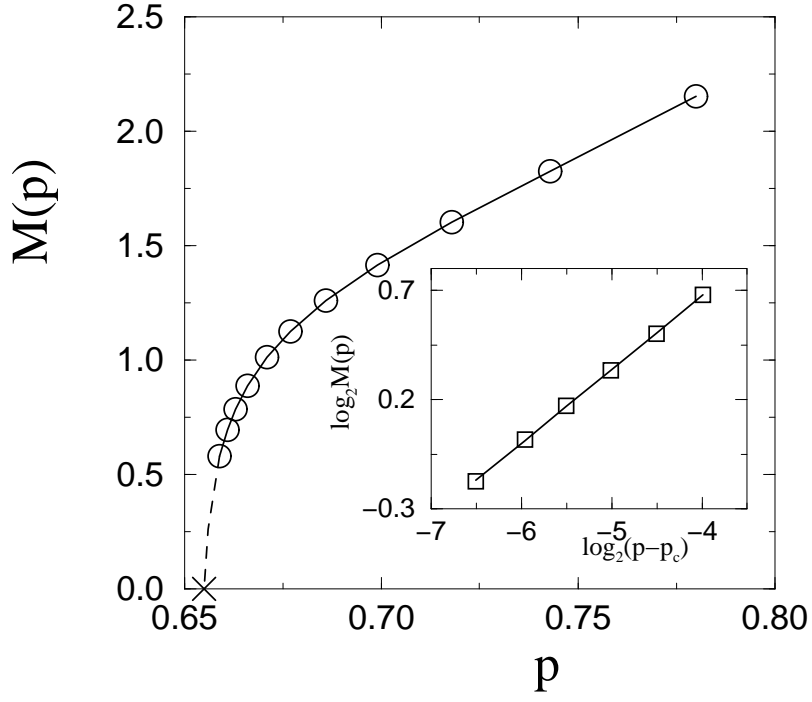
FIG. 2: Plot of spontaneous magnetization $M(p)$ against p for DSP model defined on a square lattice of size $L = 1024$. Percolation threshold p_c is marked by a cross on the p axis. In the inset, M is plotted with $(p - p_c)$. From the slope, the exponent β is obtained as ≈ 0.32.
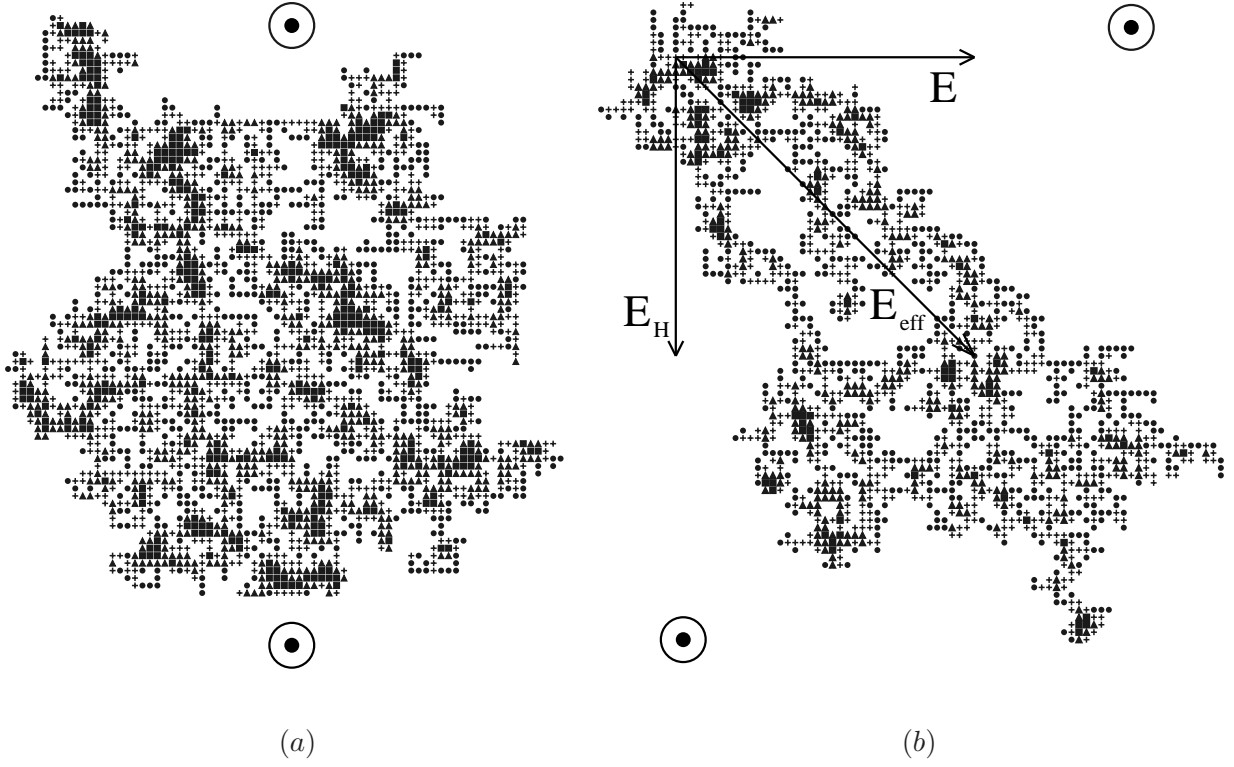
FIG. 3: Typical spanning clusters at $p = p_c$ on the square lattice of size $L = 2^6$ (a) for SP and (b) for DSP models. The encircled dots represent the rotational field B and the arrows represent the directional field E. Different symbols in the clusters represent different values of s_i as ($\bullet$) for $s_i = 1$, ($+$) for $s_i = 2$, ($\blacktriangle$) for $s_i = 3$ and ($\blacksquare$) for $s_i = 4$. The empty white space represents $s_i = 0$. It can be seen that the state variable is randomly distributed over the fractal spanning clusters.
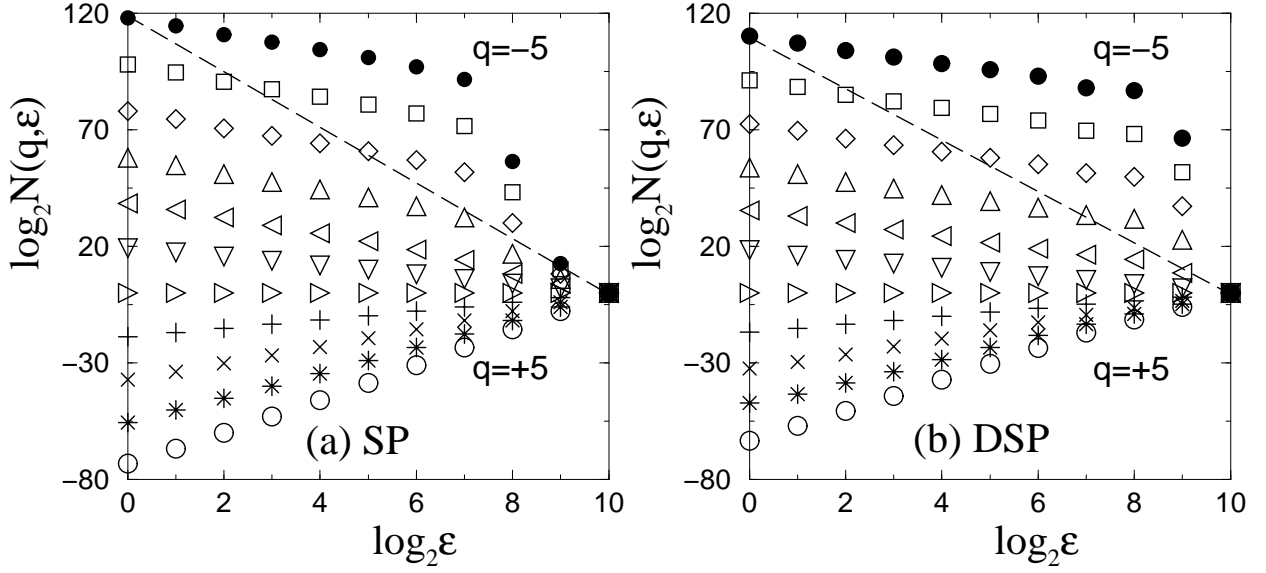
FIG. 4: Plot of weighted number of box $N(q, \epsilon)$ versus the box size ϵ for $q = -5$ to $q = 5$ in step of 1 for SP in (a) and for DSP in (b) for the spanning clusters generated on the square lattice of size $L = 1024$. The symbols are: ($\bullet$) for $q = -5$, ($\square$) for $q = -4$, ($\diamond$) for $q = -3$, ($\triangle$) for $q = -2$, ($\triangleleft$) for $q = -1$, ($\triangledown$) for $q = 0$, ($\triangleright$) for $q = 1$, ($+$) for $q = 2$, ($\times$) for $q = 3$, ($\ast$) for $q = 4$, and ($\circ$) for $q = 5$. It can be seen that box counting method is not working for $q < 0$. The expected behaviour is shown by dashed lines for $q = -5$ in both (a) and (b).
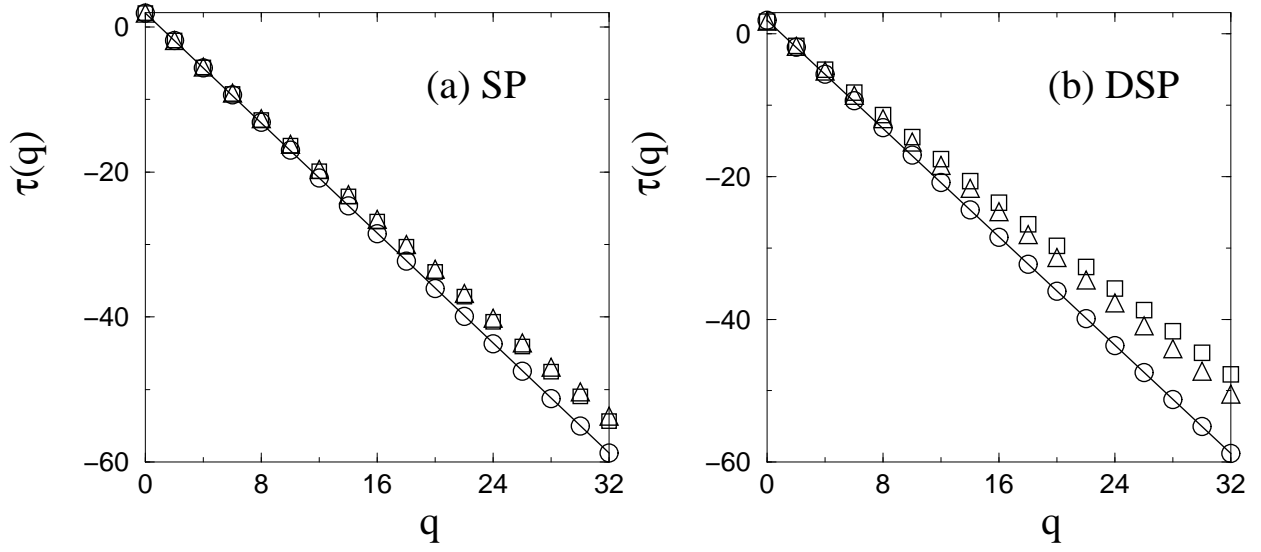
FIG. 5: Plot of the state exponent $\tau(q)$ versus the moment q for SP in (a) and for DSP in (b) for $q \geq 0$. Squares represent the square lattice data and triangles represent triangular lattice data respectively. Circles represent data of OP spanning clusters on a square lattice. The solid straight line represents the linear dependence of $\tau(q)$ on q expressed in Eq.4 for OP. The measured values of $\tau(q)$ for OP follows the straight line behaviour. For DSP and SP, $\tau(q)$ has a non-linear dependence on the moment q.
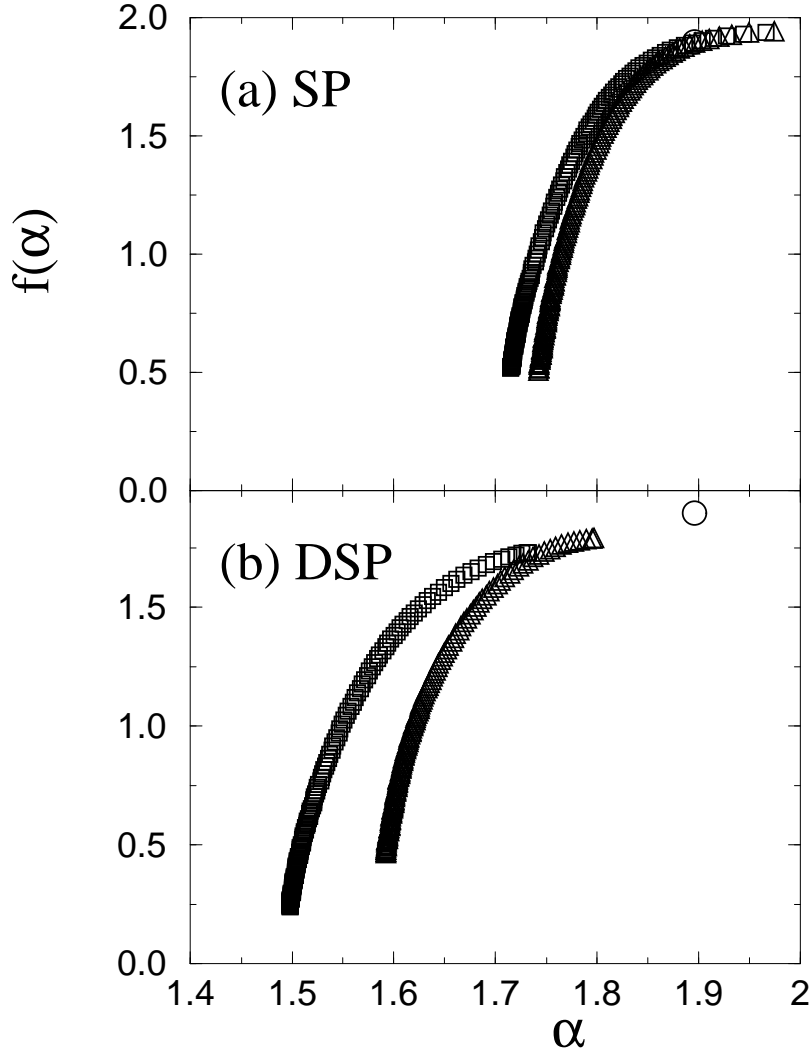
FIG. 6: Plot of fractal dimension $f(\alpha)$ against the Lipschitz-Hölder exponent α for SP (a) and DSP (b). Squares represent the square lattice data and triangle represent triangular lattice data respectively. For OP, it is a single point at $f(\alpha) = \alpha = d_f$ and represented by a circle. For DSP and SP, different spectra of $f(\alpha)$s are obtained. The spectra on the square and triangle lattice differ considerably for DSP whereas for SP they are almost identical.